LETTERS

# Complete quantum control of a single quantum dot spin using ultrafast optical pulses

David Press[1], Thaddeus D. Ladd[1,2], Bingyang Zhang[1] & Yoshihisa Yamamoto[1,2]

**A basic requirement for quantum information processing systems is the ability to completely control the state of a single qubit[1–6]. For qubits based on electron spin, a universal single-qubit gate is realized by a rotation of the spin by any angle about an arbitrary axis. Driven, coherent Rabi oscillations between two spin states can be used to demonstrate control of the rotation angle. Ramsey interference, produced by two coherent spin rotations separated by a variable time delay, demonstrates control over the axis of rotation. Full quantum control of an electron spin in a quantum dot has previously been demonstrated using resonant radio-frequency pulses that require many spin precession periods[7–10]. However, optical manipulation of the spin allows quantum control on a picosecond or femtosecond timescale[11–18], permitting an arbitrary rotation to be completed within one spin precession period[6]. Recent work in optical single-spin control has demonstrated the initialization of a spin state in a quantum dot[19–22], as well as the ultrafast manipulation of coherence in a largely unpolarized single-spin state[17]. Here we demonstrate complete coherent control over an initialized electron spin state in a quantum dot using picosecond optical pulses. First we vary the intensity of a single optical pulse to observe over six Rabi oscillations between the two spin states; then we apply two sequential pulses to observe high-contrast Ramsey interference. Such a two-pulse sequence realizes an arbitrary single-qubit gate completed on a picosecond timescale. Along with the spin initialization and final projective measurement of the spin state, these results demonstrate a complete set of all-optical single-qubit operations.**

Coherent control of a single qubit is often accomplished by driving the qubit at its resonant frequency. For a qubit composed of a single electron spin in a magnetic field, resonant coherent control requires the use of radio-frequency pulses of at least nanosecond duration[7–10]. One way to reduce this timescale is to construct qubits of multiple, coupled particles and to rapidly manipulate their coupling potential, as exemplified by the several-hundred-picosecond gate times of exchange-coupled electron pairs in electrically controlled quantum dots[23]. For an isolated, optically controlled quantum dot spin such as the one studied here, even shorter operation times may be achieved using ultrafast optical pulses[11–18]. Using such optical pulses, the axis of rotation of the qubit is determined by the arrival time of the pulse with respect to the qubit oscillation period[6]. A single-qubit gate consisting of an arbitrary rotation about any axis may thereby be completed in a single Larmor period. For electron spin qubits, a large magnetic field is therefore necessary to increase the speed of a single-qubit gate, and quantum information processing with clock speeds in excess of 10 GHz may be possible[6].

Our scheme to rotate a single electron spin using a picosecond pulse is shown in Fig. 1a. A single electron is confined in the quantum dot. The electron spin states $|\downarrow\rangle$ and $|\uparrow\rangle$ are split by an externally applied magnetic field $B_{\mathrm{ext}} = 7$ T, aligned parallel to the $z$ axis (Voigt geometry; see Fig. 1d), to provide a large Larmor precession frequency of $\delta_e/2\pi = 26.3$ GHz. The lowest energy interband transitions are to the two trion states consisting of a pair of electrons in a spin singlet and an unpaired heavy hole[24], denoted $|\uparrow\downarrow, \Downarrow\rangle$ and $|\uparrow\downarrow, \Uparrow\rangle$, which are split by a frequency $\delta_h$. Each trion state forms an independent $\Lambda$ system with the two metastable states $|\downarrow\rangle$ and $|\uparrow\rangle$. Optical selection rules dictate that the vertical and cross transitions in Fig. 1a couple to orthogonal linear polarizations of light, denoted H and V, and are $\pi/2$ out of phase with each other. The exact orientations of H and V are determined by the shape and strain of the quantum dot[25]. Each transition has a Rabi frequency $\Omega_H = \mu E_H/\hbar$ or $\Omega_V = \mu E_V/\hbar$, where $\mu$ is the transition's dipole strength and $E_H$ and $E_V$ are the complex electric field amplitudes of the rotation pulse in the corresponding polarization basis. A circularly polarized rotation pulse ensures that the probability amplitudes from the two $\Lambda$ systems add constructively, and a large detuning $\Delta$ minimizes undesired population in the excited states. Hence, a single broadband rotation pulse will coherently change the spin from $|\downarrow\rangle$ to $|\uparrow\rangle$ and back through a stimulated Raman transition. The dynamics may be qualitatively described by the condition that $\Omega_H \ll \Delta$ and $\Omega_V \ll \Delta$, under which the upper levels can be adiabatically eliminated. Doing so, we expect to find two-state Rabi oscillations with an effective Rabi frequency $\Omega_{\mathrm{eff}} \approx \Omega_H\Omega_V/\Delta$ between states $|\downarrow\rangle$ and $|\uparrow\rangle$. The spin rotation may alternatively be described in terms of an optical Stark shift[17].

In addition to rotations, a complete set of single-qubit operations also requires initialization and measurement. We perform both of these tasks by optical pumping (Fig. 1b). A narrowband, continuous-wave laser optically drives the $|\downarrow\rangle \leftrightarrow |\uparrow\downarrow, \Downarrow\rangle$ transition with rate $\Omega_P$. The optical pumping laser has negligible effect on the spin rotation because $\Omega_P \ll \Omega_{\mathrm{eff}}$. Spontaneous decay into the two spin states at half the trion's total spontaneous emission rate, denoted $\Gamma$, quickly initializes the electron into the $|\uparrow\rangle$ state. After spin rotation, the population in the $|\downarrow\rangle$ state is measured using the same optical pumping process. If the spin is rotated to $|\downarrow\rangle$, the quantum dot will emit a single photon from the $|\uparrow\downarrow, \Downarrow\rangle \rightarrow |\uparrow\rangle$ transition, which can be detected using a single-photon counter.

Our single-spin measurement technique has been proposed for use in quantum computation[1], and offers the experimental convenience of including measurement and initialization in the same step. However, the fidelity of a single-shot readout is limited by the photon collection efficiency. An optical microcavity would boost the measurement scheme's efficiency, and could also enable coherent conversion of spin qubits into photon qubits for quantum networking[26]. Resonant absorption measurements[19–21] offer similar advantages, but also require a microcavity-enhanced absorption cross-section to enable single-shot readout. Quantum non-demolition measurements based on dispersive Kerr rotation[27], Faraday rotation[28] or a recycling transition[29] use many photons to measure the spin and are therefore more robust to photon loss, but they require a separate initialization step.

[1]E. L. Ginzton Laboratory, Stanford University, Stanford, California 94305, USA. [2]National Institute of Informatics, Hitotsubashi 2-1-2, Chiyoda-ku, Tokyo 101-8403, Japan.

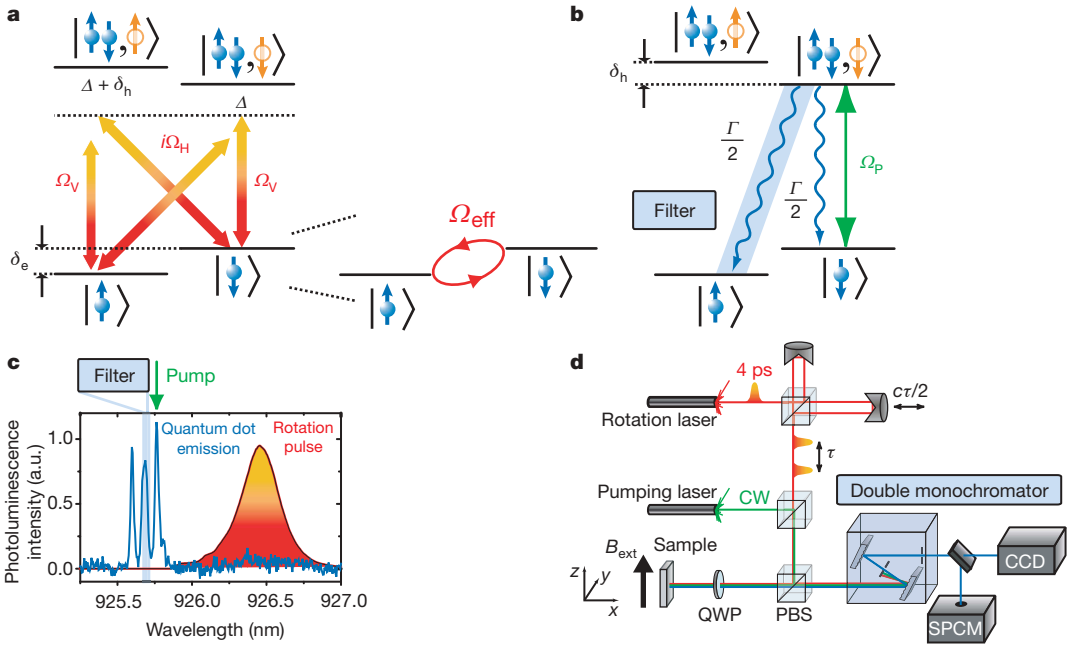


**Figure 1 | Experimental methods to initialize, control and measure a single electron spin.** **a**, The spin rotation scheme involves a stimulated Raman transition through two independent Λ systems. The four-level system is effectively reduced to a two-level system if the Rabi frequencies, $\Omega_H$ and $\Omega_V$, are much smaller than the detuning, $\Delta$. **b**, The spin initialization and measurement scheme performed by optical pumping. **c**, Measured photoluminescence spectrum of the charged quantum dot excited by an above-bandgap, 785-nm laser. The rotation pulse is detuned by $\Delta/2\pi = 290$ GHz below the lowest transition frequency. **d**, Experimental set-up. During each experimental cycle, one or two rotation pulses may be sent to the sample to observe Rabi oscillations or Ramsey interference, respectively. The time delay, $\tau$, between pairs of pulses is controlled by a retroreflector mounted on a computer-controlled translation stage. CW, continuous wave; QWP, quarter-wave plate; PBS, polarizing beam splitter; SPCM, single-photon counting module; CCD, charge-coupled device; $c$, speed of light.

The optical initialization is calibrated by measuring the single-photon count rate as a function of optical pumping power, $P_{OP}$, following a fixed rotation through angle $\Theta = \pi$ (Fig. 2a). The signal saturates at around $P_{OP} \approx 15\,\mu W$ as the population in the $|\downarrow\rangle$ state becomes almost completely initialized to $|\uparrow\rangle$. In all of our remaining experiments, $P_{OP}$ is fixed just above the saturation value of the optical pumping curve. To quantify the initialization fidelity, we make a time-resolved measurement of photon count rate following a rotation of $\Theta = \pi$ (Fig. 2b). The count rate is proportional to the instantaneous population in $|\downarrow\rangle$. Immediately following the rotation pulse, the population in $|\downarrow\rangle$ is near unity and the signal is maximized. The signal drops as the spin is pumped back to $|\uparrow\rangle$ in a characteristic time of 3.4 ns, orders of magnitude faster[21] than optical pumping schemes involving a dipole-forbidden transition[19]. The minimum count rate, which is measured just before the next rotation pulse, corresponds to the remnant population in $|\downarrow\rangle$ due to imperfect initialization. By comparing the count rates immediately before and after the rotation pulse, we estimate (see Supplementary Information) the spin initialization fidelity to be $F_0 = 92 \pm 7\%$.

Rabi oscillations between the two spin states are evident in the photon count rate as the rotation pulse power $P_{RP}$ is varied (Fig. 3a). By contrast with the adiabatic-elimination model discussed earlier, in which $\Theta \propto P_{RP}$, we empirically determine that $\Theta \propto P_{RP}^{0.68}$ in the range $\pi \leq \Theta \leq 13\pi$ (Fig. 3b). This sublinear dependency is a consequence of the breakdown of the adiabatic approximation ($\Omega_H \ll \Delta$, $\Omega_V \ll \Delta$), as non-negligible virtual population is present

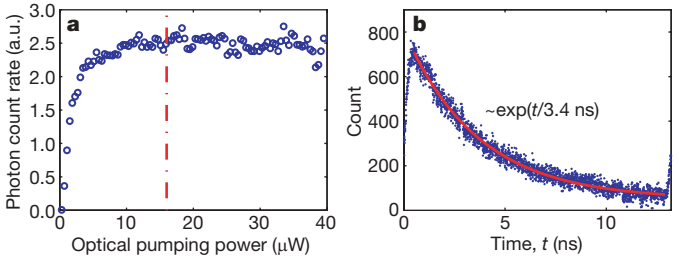


**Figure 2 | Initialization by optical pumping.** **a**, Saturation of the spin initialization process by means of optical pumping, showing single-photon signal as a function of optical pumping power for a fixed rotation angle $\Theta = \pi$. The operating power, $P_{OP}$, for the optical pump in all subsequent experiments is indicated by the dash–dot line. **b**, Time-resolved measurement of optical pumping following a fixed rotation by $\Theta = \pi$. The count rate is fitted by an exponential decay with a 3.4-ns time constant. a.u., arbitrary units.

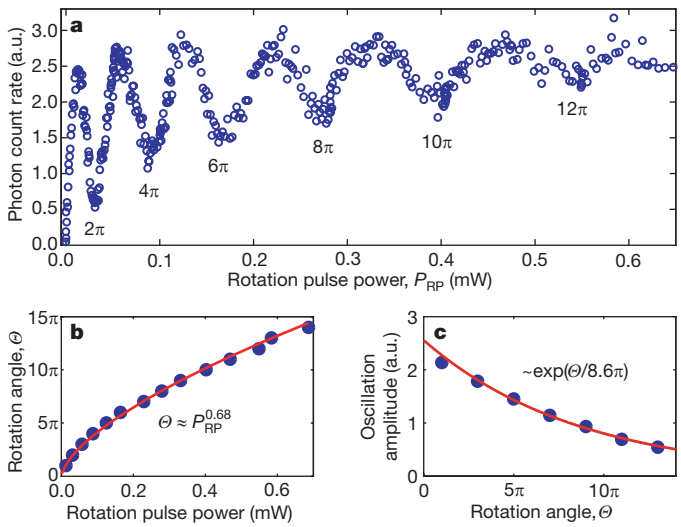


**Figure 3 | Experimental demonstration of Rabi oscillations.** **a**, Rabi oscillations between the spin states are evident in the oscillating photon signal as rotation pulse power, $P_{RP}$, is increased. **b**, The rotation angle as a function of rotation pulse power, showing an empirical fit to a power-law dependence. **c**, Amplitude of measured Rabi oscillations as a function of rotation angle, with an empirical exponential fit.

in the excited states during the rotation pulse. A four-level master-equation simulation of stimulated Raman scattering with no adjustable parameters and no decoherence processes (see Supplementary Information) produces oscillations that are well fit by $\Theta \propto P_{RP}^{0.65}$, in reasonable agreement with experiment.

The amplitude of the Rabi oscillations shrinks owing to incoherent processes such as trion dephasing. This may be understood as a decrease of the length of the Bloch vector of the two-state system as $\Theta$ increases. This decreasing length is well fit (excluding the first data point) by an empirical exponential decay proportional to $\exp(-\Theta/8.6\pi)$, as shown in Fig. 3c. These incoherent processes transform the virtual population in the excited states during the rotation pulse into real population, which contributes to the photon count rate as background noise. The increasing background is responsible for the overall upwards slope of the data in Fig. 3a.

The experimentally determined trajectory of the Bloch vector as it undergoes Rabi oscillations is parametrically plotted in Fig. 4 as a function of rotation pulse power. The methods we used to generate this trajectory are described in the Supplementary Information. For small rotation angles $\Theta \lesssim \pi$, the vector rotates about a tilted axis because the Larmor precession frequency, $\delta_e$, is non-negligible in comparison with the effective Rabi frequency, $\Omega_{eff}$. This tilted axis of rotation causes the reduction in height of the first peak in Fig. 3a and the lowering of the first oscillation amplitude in Fig. 3c. For larger rotation angles, $\Omega_{eff} \gg \delta_e$ and the rotation is very nearly about the $x$ axis.

Rabi oscillations demonstrate the rotation of a qubit by an arbitrary angle about a single axis, that is, U(1) control. Full control over the Bloch sphere (SU(2) control) requires rotation about a second axis. The natural Larmor precession of the spin about the $z$ axis accomplishes this rotation, and can be investigated using Ramsey interferometry.

In a Ramsey interferometer, the spin population is measured following a pair of $\pi/2$ rotations about the $x$ axis separated by a variable free precession of time $\tau$ about the $z$ axis. Ramsey fringes are shown in Fig. 5a. The fringe amplitude decays with a time constant $T_2^* = 185$ ps. This small time constant is a consequence of the optical pumping laser remaining on between the two rotation pulses, and could be increased by switching the optical pump off between pulses using a fast electro-optic modulator. We determine the electron $g$-factor magnitude to be $|g_e| = 0.267$ from the Larmor frequency $\delta_e/2\pi = 26.3$ GHz. To estimate the fidelity of each $\pi/2$ pulse, we assume that the Bloch vector initially has length $L_0 = 0.83$ (determined from our initialization fidelity of 92%) and is directed towards the south pole of the Bloch sphere, and that it shrinks in length by a factor of $D_{\pi/2}$ with each pulse. The Bloch vector length after two pulses is thus $L_0 D_{\pi/2}^2$, and the population in state $|\downarrow\rangle$ oscillates between $(1 + L_0 D_{\pi/2}^2)/2$ and $(1 - L_0 D_{\pi/2}^2)/2$ with a Larmor period of $2\pi/\delta_e$. The fidelity of each rotation is then given by $(1 + D_{\pi/2})/2$. We estimate the fidelity by considering the Ramsey fringe amplitude at the shortest measured delay time (see Supplementary Information for details). This gives a $\pi/2$ pulse fidelity of $F_{\pi/2} = 94\%$.

To investigate the quality of our $\pi$ pulses, we perform a similar experiment with two $\pi$ pulses separated by a variable time delay, as shown in Fig. 5b. Ideally, the signal would remain constant at $L_0(1 - D_\pi^2)/2$ with no oscillations. The signal shows an overall upwards slope, again due to the optical pump remaining on between the two $\pi$ pulses and pumping population from the $|\downarrow\rangle$ state into $|\uparrow\downarrow, \Downarrow\rangle$ where it is later detected. Small oscillations remain in the signal because our $\pi$ pulse is not exactly around the $x$ axis, as discussed earlier. We estimate from the phase of these remaining fringes that our $\pi$ pulse rotates the spin about a vector tilted 0.17 rad from the $x$ axis. If we simply model the rotation pulse as a rectangular pulse with constant frequency $\Omega_{eff}$ applied over 4 ps, we would expect to rotate around an axis tilted by roughly $\delta_e/\Omega_{eff} = 0.21$ rad, in reasonable agreement with experiment. By comparing the length and orientation of the Bloch vector after our $\pi$ pulse with a unit vector in the direction of the north pole of the Bloch sphere, we estimate our $\pi$ pulse fidelity to be roughly $F_\pi = 91\%$.

To construct a general SU(2) single-qubit gate, we may adjust the intensities of the first and second rotation pulses and the precession duration, $\tau$, thus applying three rotations through Euler angles about the $x$, $z$ and $x$ axes. In Fig. 5c we explore the entire surface of the Bloch sphere by varying the rotation angle of both rotation pulses as well as the delay time $\tau$. The fringe amplitude is shown as a function of rotation angle in Fig. 5d. High-contrast Ramsey fringes are visible when each rotation angle is a half-integer multiple of $\pi$, and the fringes vanish when each rotation angle is an integer multiple of $\pi$.

In conclusion, we have demonstrated the optical initialization, rotation by arbitrary angle, and projective measurement of an electron spin in a quantum dot. This forms a complete set of all-optical single-qubit operations. A single-qubit gate, consisting of three independent rotations about different axes, is accomplished in less than one Larmor period of 38 ps. Coherence times of $T_2 = 3.0$ μs have

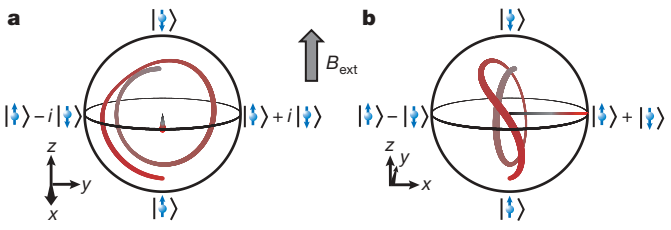


**Figure 4 | Reconstructed evolution of the Bloch vector.** The curves trace out the tip of the Bloch vector in the one-pulse (Rabi oscillation) experiment over the range of rotation angles $0 \le \Theta \le 3\pi$. The colour scale indicates the length of the Bloch vector, which shrinks exponentially with $\Theta$. Views are from the perspective of the $x$ axis (**a**) and the $-y$ axis (**b**) of the Bloch sphere. The rotation angle and the length of the Bloch vector are extracted from the extrema of the Rabi oscillation data shown in Fig. 3, and the azimuthal position of the Bloch vector is determined from the phase of the Ramsey fringes shown in Fig. 5.

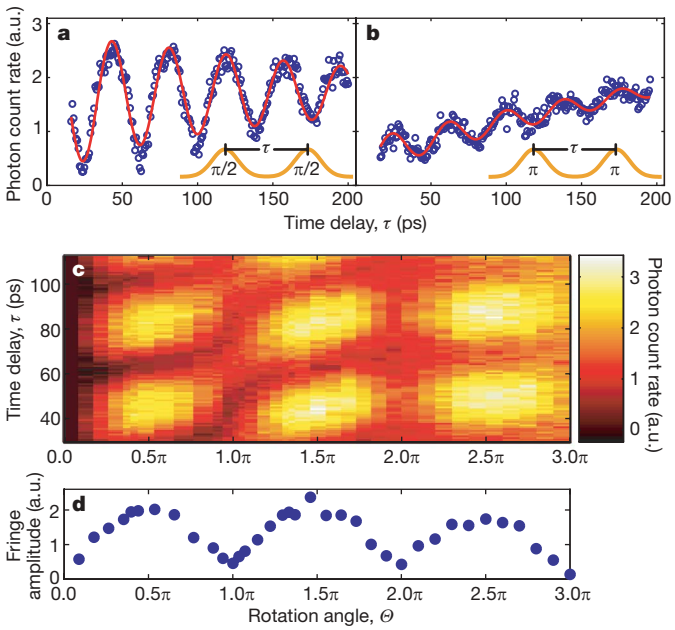


**Figure 5 | Experimental demonstration of Ramsey fringes.** **a**, Ramsey interference for a pair of $\pi/2$ pulses, showing photon count rate as a function of the time delay between pulses. **b**, Ramsey fringes for a pair of $\pi$ pulses. The data in **a** and **b** are fitted to an exponentially decaying sinusoid with a linear offset (see Supplementary Information for details). **c**, Photon count rate is colour-mapped as a function of rotation angle, $\Theta$, and delay time between pulses, $\tau$. **d**, The amplitude of Ramsey fringes for various rotation angles. Fringe amplitudes are determined by fitting the data shown in **c** with decaying sinusoids.

been reported for quantum dot electron spins[13], so nearly $10^5$ gate operations may be possible within the qubit's coherence time. The rotation pulses are of sufficient fidelity to be applied to a simple spin-based quantum information processing system. Our results are also readily applicable to a spin–photon interface for quantum networks, and suggest methods of greatly increasing the speed and number of operations in general spin-based quantum information processing schemes.

## METHODS SUMMARY

The sample contained about $5 \times 10^9\ \mathrm{cm}^{-2}$ self-assembled InGaAs quantum dots grown by the Stranski–Krastanow method on a GaAs substrate. A $\delta$-doping layer of Si donors with a surface density of roughly $10^{10}\ \mathrm{cm}^{-2}$ was grown 20 nm below the layer of quantum dots to probabilistically dope them. Roughly half of the quantum dots were charged, and could be identified by their splitting into a symmetrical quadruplet at high magnetic field (Fig. 1c). The sample was etched into 600-nm-diameter mesa structures containing roughly ten quantum dots that could be individually spectroscopically probed.

The experimental setup is shown in Fig. 1d. The sample was cooled to 1.5 K in a superconducting magnetic cryostat. The optical pumping and rotation pulse lasers were focused onto the sample using an aspheric objective lens (numerical aperture of 0.68) placed inside the cryostat. The sample was positioned relative to the objective using piezoelectric 'slip-stick' positioners. Single-photon photoluminescence was collected through the same lens and directed onto a single-photon counter or charge-coupled device. Collection efficiency was further enhanced using a hemispherical solid immersion lens. The quantum dot emission was spectrally dispersed and filtered using a double monochromator with 0.02-nm resolution. Scattered laser light was further rejected by double-passing through a quarter-wave plate and polarizer. The optical pumping laser was tuned to be resonant with the lowest energy excitonic transition, and the rotation pulse laser was detuned by $\Delta/2\pi = 290$ GHz below the lowest transition frequency. The rotation pulse laser was modulated at 500 Hz using an optical chopper, and the signal from the single-photon counter was detected using a lock-in amplifier. For the time-resolved measurement (Fig. 2b), a timing histogram was generated using a time-interval analyser without lock-in amplification. Instead, the background from scattered optical pump photons and detector dark counts was independently measured and subtracted.

**Received 1 July; accepted 6 October 2008.**


1. Imamoglu, A. *et al.* Quantum information processing using quantum dot spins and cavity QED. *Phys. Rev. Lett.* **83,** 4204–4207 (1999).
2. Combescot, M. & Betbeder-Matibet, O. Theory of spin precession monitored by laser pulse. *Solid State Commun.* **132,** 129–134 (2004).
3. Chen, P., Piermarocchi, C., Sham, L. J., Gammon, D. & Steel, D. G. Theory of quantum optical control of a single spin in a quantum dot. *Phys. Rev. B* **69,** 075320 (2004).
4. Pryor, C. E. & Flatté, M. E. Predicted ultrafast single-qubit operations in semiconductor quantum dots. *Appl. Phys. Lett.* **88,** 233108 (2006).
5. Economou, S. E., Sham, L. J., Wu, Y. & Steel, D. G. Proposal for optical U(1) rotations of electron spin trapped in a quantum dot. *Phys. Rev. B* **74,** 205415 (2006).
6. Clark, S. M., Fu, K.-M. C., Ladd, T. D. & Yamamoto, Y. Quantum computers based on electron spins controlled by ultrafast off-resonant single optical pulses. *Phys. Rev. Lett.* **99,** 040501 (2007).
7. Koppens, F. H. L. *et al.* Driven coherent oscillations of a single electron spin in a quantum dot. *Nature* **442,** 766–771 (2006).
8. Tokura, Y., van der Wiel, W., Obata, T. & Tarucha, S. Coherent single electron spin control in a slanting Zeeman field. *Phys. Rev. Lett.* **96,** 047202 (2006).
9. Nowack, K. C., Koppens, F. H. L., Nazarov, Y. V. & Vandersypen, L. M. K. Coherent control of a single electron spin with electric fields. *Science* **318,** 1430–1433 (2007).
10. Koppens, F. H. L., Nowack, K. C. & Vandersypen, L. M. K. Spin echo of a single electron spin in a quantum dot. *Phys. Rev. Lett.* **100,** 236802 (2008).
11. Gupta, J. A., Knobel, R., Samarth, N. & Awschalom, D. D. Ultrafast manipulation of electron spin coherence. *Science* **292,** 2458–2461 (2001).
12. Dutt, M. V. G. *et al.* Ultrafast optical control of electron spin coherence in charged GaAs quantum dots. *Phys. Rev. B* **74,** 125306 (2006).
13. Greilich, A. *et al.* Mode locking of electron spin coherences in singly charged quantum dots. *Science* **313,** 341–345 (2006).
14. Wu, Y. *et al.* Selective optical control of electron spin coherence in singly charged GaAs-$Al_{0.3}Ga_{0.7}$As quantum dots. *Phys. Rev. Lett.* **99,** 097402 (2007).
15. Greilich, A. *et al.* Robust manipulation of electron spin coherence in an ensemble of singly charged quantum dots. *Phys. Rev. B* **75,** 233301 (2007).
16. Carter, S. G., Chen, Z. & Cundiff, S. T. Ultrafast below-resonance Raman rotation of electron spins in GaAs quantum wells. *Phys. Rev. B* **76,** 201308(R) (2007).
17. Berezovsky, J., Mikkelson, M. H., Stoltz, N. G., Coldren, L. A. & Awschalom, D. D. Picosecond coherent optical manipulation of a single electron spin in a quantum dot. *Science* **320,** 349–352 (2008).
18. Fu, K.-M. C. *et al.* Ultrafast control of donor-bound electron spins with single detuned optical pulses. *Nature Phys.* **4,** 780–784 (2008).
19. Atatüre, M. *et al.* Quantum-dot spin-state preparation with near-unity fidelity. *Science* **312,** 551–553 (2006).
20. Gerardot, B. D. *et al.* Optical pumping of a single hole spin in a quantum dot. *Nature* **451,** 441–443 (2008).
21. Xu, X. *et al.* Fast spin state initialization in a singly charged InAs-GaAs quantum dot by optical cooling. *Phys. Rev. Lett.* **99,** 097401 (2007).
22. Ramsay, A. J. *et al.* Fast optical preparation, control, and readout of a single quantum dot spin. *Phys. Rev. Lett.* **100,** 197401 (2008).
23. Petta, J. R. *et al.* Coherent manipulation of coupled electron spins in semiconductor quantum dots. *Science* **309,** 2180–2184 (2005).
24. Bayer, M. *et al.* Fine structure of neutral and charged excitons in self-assembled In(Ga)As/(Al)GaAs quantum dots. *Phys. Rev. B* **65,** 195315 (2002).
25. Krizhanovskii, D. N. *et al.* Individual neutral and charged $In_xGa_{1-x}As$-GaAs quantum dots with strong in-plane optical anisotropy. *Phys. Rev. B* **72,** 161312(R) (2005).
26. Cirac, J. I., Zoller, P., Kimble, H. J. & Mabuchi, H. Quantum state transfer and entanglement distribution among distant nodes in a quantum network. *Phys. Rev. Lett.* **78,** 3221–3224 (1997).
27. Berezovsky, J. *et al.* Nondestructive optical measurements of a single electron spin in a quantum dot. *Science* **314,** 1916–1920 (2006).
28. Atatüre, M., Dreiser, J., Badolato, A. & Imamoglu, A. Observation of Faraday rotation from a single confined spin. *Nature Phys.* **3,** 101–105 (2007).
29. Shabaev, A., Efros, A. L., Gammon, D. & Merkulov, I. A. Optical readout and initialization of an electron spin in a single quantum dot. *Phys. Rev. B* **68,** 201305(R) (2003).


**Supplementary Information** is linked to the online version of the paper at www.nature.com/nature.

**Acknowledgements** This work was supported by JST/SORST, NICT, MEXT, MURI (ARMY, DAAD 19-03-1-0199) and Special Coordination Funds for Promoting Science and Technology. We thank S. Koseki, S. Götzinger, C. Santori and Q. Zhang for their assistance.

**Author Information** Reprints and permissions information is available at www.nature.com/reprints. Correspondence and requests for materials should be addressed to D.P. (dlpress@stanford.edu).